Uts2b is a microbiota-regulated gene expressed in vagal afferent neurons connected to enteroendocrine cells producing cholecystokinin

Yoshioka, Yuta ; Tachibana, Yoshihisa ; Uesaka, Toshihiro ; Hioki, Hiroyuki ; Sato, Yuya ; Fukumoto, Takumi ; Enomoto, Hideki

(Citation)
Biochemical and Biophysical Research Communications,608:66-72

(Issue Date)
2022-06-11

(Resource Type)
journal article

(Version)
Version of Record

(URL)
https://hdl.handle.net/20.500.14094/90009216

Biochemical and Biophysical Research Communications 608 (2022) 66–72

Contents lists available at ScienceDirect

Biochemical and Biophysical Research Communications

journal homepage: www.elsevier.com/locate/ybbrc

Uts2b is a microbiota-regulated gene expressed in vagal afferent neurons connected to enteroendocrine cells producing cholecystokinin

Yuta Yoshioka [a], Yoshihisa Tachibana [b], Toshihiro Uesaka [a], Hiroyuki Hioki [c], Yuya Sato [a], Takumi Fukumoto [d], Hideki Enomoto [a, *]

[a] Division for Neural Differentiation and Regeneration, Department of Physiology and Cell Biology, Kobe University Graduate School of Medicine, Kobe, Japan
[b] Department of Physiology and Cell Biology, Kobe University Graduate School of Medicine, Kobe, Japan
[c] Department of Neuroanatomy, Juntendo University Graduate School of Medicine, Bunkyo-Ku, Tokyo, Japan
[d] Division of Hepato-Biliary-Pancreatic Surgery, Department of Gastroenterological Surgery, Kobe University Graduate School of Medicine, Kobe, Japan

ARTICLE INFO

Article history:
Received 8 March 2022
Accepted 23 March 2022
Available online 31 March 2022

Keywords:
Gut-brain axis
Nodose ganglion
Vagal afferent neurons
Microbiota
Uts2b

ABSTRACT

Enteroendocrine cells (EECs) are the primary sensory cells that sense the gut luminal environment and secret hormones to regulate organ function. Recent studies revealed that vagal afferent neurons are connected to EECs and relay sensory information from EECs to the brain stem. To date, however, the identity of vagal afferent neurons connected to a given EEC subtype and the mode of their gene responses to its intestinal hormone have remained unknown. Hypothesizing that EEC-associated vagal afferent neurons change their gene expression in response to the microbiota-related extracellular stimuli, we conducted comparative gene expression analyses of the nodose-petrosal ganglion complex (NPG) using specific pathogen-free (SPF) and germ-free (GF) mice. We report here that the *Uts2b* gene, which encodes a functionally unknown neuropeptide, urotensin 2B (UTS2B), is expressed in a microbiota-dependent manner in NPG neurons. In cultured NPG neurons, expression of *Uts2b* was induced by AR420626, the selective agonist for FFAR3. Moreover, distinct gastrointestinal hormones exerted differential effects on *Uts2b* expression in NPG neurons, where cholecystokinin (CCK) significantly increased its expression. The majority of *Uts2b*-expressing NPG neurons expressed CCK-A, the receptor for CCK, which comprised approximately 25% of all CCK-A-expressing NPG neurons. Selective fluorescent labeling of *Uts2b*-expressing NPG neurons revealed a direct contact of their nerve fibers to CCK-expressing EECs. This study identifies the *Uts2b* as a microbiota-regulated gene, demonstrates that *Uts2b*-expressing vagal afferent neurons transduce sensory information from CCK-expressing EECs to the brain, and suggests potential involvement of UTS2B in a modality of CCK actions.

1. Introduction

Gut-Brain axis plays a central role in metabolic homeostasis. Enteroendocrine cells (EECs) are gut sensor cells that express a variety of receptors to sense nutrients and chemical substances in the gut luminal environment [1,2], which is established by microbiota-host interactions. In response to those environmental cues, EECs secret intestinal hormones and regulate organ function. Recent studies revealed that some EECs form synapses with the nerves of vagal afferent neurons at their basal protrusions called 'neuropod' and undergo neurotransmission [3,4]. Those vagal afferent neurons relay gut sensory information from EECs to the brain stem, which leads to the alteration of metabolism-related animal behavior such as appetite, satiety and nutrient preference [5,6].

In mice, EECs producing serotonin, peptide YY (PYY), CCK, or glucagon-like peptide 1 (GLP-1) have been reported to form synaptic connections with vagal afferent nerves [3,4]. On the other hand, mouse vagal afferent neurons are genetically classified into

* Corresponding author. Division for Neural Differentiation and Regeneration, Department of Physiology and Cell Biology, Kobe University Graduate School of Medicine, 7-5-1 Kusunoki-cho, Chuo-ku, Kobe, Hyogo, 650-0017, Japan.
E-mail address: enomotoh@med.kobe-u.ac.jp (H. Enomoto).

https://doi.org/10.1016/j.bbrc.2022.03.117

twelve subtypes, and at least three subtypes innervate to the gut mucosa [7]. These mucosa-innervating neurons are considered to monitor gut luminal environment directly by sensing nutrients and indirectly by responding to EEC-derived signals including neurotransmitters and intestinal hormones. The exact identity of vagal afferent neurons that connected to a given EEC subtype and how those neurons respond to the intestinal hormones, however, have remained unclear.

Intestinal hormones and many nutrients signal through G-protein coupled receptors (GPCR). In many cell types, the activation of GPCR initiate intracellular cell signaling cascades, which causes changes in gene expression [8]. We hypothesized that EEC-associated vagal afferent neurons change their gene expression in response to microbiota-associated extracellular stimuli such as bacterial metabolites and intestinal hormones. To identify such genes, we performed comparative gene expression analyses of the nodose-petrosal ganglion complex (NPG) of SPF and germ-free (GF) mice.

2. Methods

2.1. Reagents

AR420626 and Pam3CSK4 were purchased from Thermo Fisher. Lipopolysaccharide (LPS) was purchased from Sigma-Aldrich. CCK-8, PYY, and Glucagon-like Peptide 1 were purchased from Peptide Institute.

2.2. Animal experiments

C57BL/6 N female mice were obtained from CLEA Japan. Mice were kept under specific pathogen-free (SPF) conditions, and were housed in a temperature-controlled environment with a 12 h light/12 h dark cycle with access to food and water *ad libitum*. Female germ-free (GF) mice on a C57BL/6 N background were purchased from CLEA Japan, Inc. (Tokyo, Japan). To conventionalize GF mice (CONV-D mice), feces derived from age- and sex-matched SPF mice were suspended in distilled water and transplanted into 3-weeks-old GF mice by oral gavage. *Vip-IRES-Cre* (#010908) [9], *RCFL-tdT* (Ai65; # 021875), and *Slc17a6-Flpo* (#030212) mice were purchased from Jackson laboratories. All experimental procedures were approved by the Institutional Animal Care and Use Committee, and carried out in compliance with the Kobe University Animal Experimentation Regulations.

2.3. Quantitative real-time polymerase chain reaction (qRT-PCR)

Total RNAs were isolated from the nodose-petrosal ganglion complex (NPG) of SPF and GF mice with TRIzol reagent (Thermo Fisher). 20 ng of total RNAs were reverse-transcribed with CellAmp Whole Transcriptome Amplification Kit (Real Time) Ver.2 (Takara Bio, Japan) by oligo(dT) primers, and then used as templates for qRT-PCR with KAPA SYBR Fast qPCR kit (NIPPON genetics, Japan) on a 7500 Real Time PCR System (Applied Biosystems). The primers used for qRT-PCR are described in Supplemental Table 1. The relative gene expression was calculated by the comparative $2^{-\Delta\Delta Ct}$ method. All expression data were normalized to those for *Actb*.

2.4. In situ hybridization (ISH)

ISH was performed on 16 μm cryosections of the NPG as previously described [10]. All riboprobes for ISH were synthesized using the DIG RNA Labeling Kit (Roche Diagnostics, Switzerland) as specified by the manufacturer. Digoxigenin (DIG)-labeled complementary RNA probes were generated using the primer pairs described in Supplemental Table 2. The hybridized DIG-labeled probes were detected by anti-DIG antibody conjugated with alkaline phosphatase (1:2000; Roche Diagnostics) and exposure with nitroblue tetrazolium (Roche Diagnostics) and 5-bromo-4-chloro-3-indolyl phosphate (Roche Diagnostics) color substrates.

2.5. Fluorescent in situ hybridization (FISH)

FISH was performed on 16 μm cryosections of nodose petrosal ganglia as previously described [11]. Riboprobes for FISH were synthesized by the DIG RNA Labeling Kit or the Fluorescein RNA Labeling Kit (Roche Diagnostics) using primer pairs described in Supplemental Table 3. The hybridized DIG-labeled probes were detected by HRP conjugated anti-DIG antibody (1:500 in blocking buffer) and treated with TSA-plus Cyanine 3 (PerkinElmer, NEL744001KT, 1:70 in 1x plus amplification diluent). The hybridized Fluorescein-labeled probes were detected by TSA-plus biotin (PerkinElmer, NEL749A001KT, 1:70 in 1x plus amplification diluent) and treated with streptavidin-Alexa Fluor 488 (Life Technologies, 1:250).

2.6. Immunohistochemistry

Immunohistochemistry was performed as described previously [12]. Briefly, 16 μm cryosections of the NPG were blocked with blocking solution [PBS containing 1% (w/v) bovine serum albumin (Sigma-Aldrich), 0.3% TritonX-100, and 0.2% (w/v) skim milk (BD Bioscience)] for 1 h, then incubated with primary antibody in blocking solution at 4 °C overnight. The sections were incubated with appropriate secondary antibodies for 2 h at room temperature. The antibodies used were as follows; rabbit anti-Iba1 (1:10000; RRID: AB_2832244, Abcam), rabbit anti-cholecystokinin (CCK) 26–33 (1:1000; Phoenix Pharmaceuticals), AlexaFluor®594-conjugated donkey anti-rabbit IgG (1:500; RRID: AB_141637, Thermo Fisher), AlexaFluor®488-conjugated donkey anti-rabbit IgG (1:500; RRID: AB_2535792, Thermo Fisher).

2.7. Primary culture of the NPG and their treatment with chemicals and hormones

NPG were dissected from postnatal day 0 SPF mice. For explant cultures, the isolated NPG were embedded in 1 ml of type I collagen (Rat Tail, 4.0 mg/ml; Corning) in 35 mm tissue culture dishes. After gelation, the explants were overlaid with DMEM (low glucose) with GlutaMAX supplement, supplemented with, Glutamax Supplement (Thermo Fisher) supplemented with 10% fetal bovine serum (Thermo Fisher), 2% B27 (Thermo Fisher), and 1% penicillin-streptomycin (Thermo Fisher) at 37 °C with 5% CO_2 for 48 h.

2.8. Quantitative analysis

The number of NPG neurons was manually counted in ISH, as judged by their large cell bodies (typically >500 μm^2) and large spherical nuclei (typically >13 μm in diameter) compared to other cell types (typically <200 μm^2 and <9 μm, respectively) with non-spherical nuclei. The number of riboprobe-positive neurons was calculated as a percentage of total neurons in the NPG. For *Cd74* ISH, total riboprobe-positive cells were counted because of no expression in neurons. Images were acquired by a HS All-in-one Fluorescence Microscope (Keyence). The numbers of single or double riboprobe-positive neurons per NPG were manually counted in two color FISH. Fluorescent images were acquired by a Zeiss Axioskop 2FS plus fluorescent microscope (Zeiss) or an LSM5 PASCAL laser scanning confocal microscope (Zeiss).

2.9. Statistical analysis

Statistical analysis was performed using GraphPad Prism 8 (GraphPad Software, Inc.). The Shapiro-Wilk test was used to test whether the data exhibited Gaussian distribution. All data were presented as means ± standard error of the mean (SEM) of at least three independent experiments. Comparison between individual groups was performed by Mann-Whitney *U* test and unpaired *t*-test with Welch's correction. No test for outlier was conducted on the data and no data point was excluded from the analysis.

For more details, see Supplemental materials and methods.

3. Results

To identify genes expressed in the vagal afferent neurons in a microbiota-dependent manner, we compared gene expression profiles of the nodose-petrosal ganglion (NPG) between germ-free (GF) and SPF mice, and between GF and conventionalized (CONV-D: fecal transfer from SFP to GF) mice (Supplemental Figs. 1A and B). Fifty-eight genes were selected as candidates that were expressed at higher levels in SPF and CONV-D than in GF (Supplemental Fig. 1C). Of those, expression of twenty-two genes was verified by quantitative RT-PCR analysis (qRT-PCR, Supplemental Tables 4 and 5) followed by

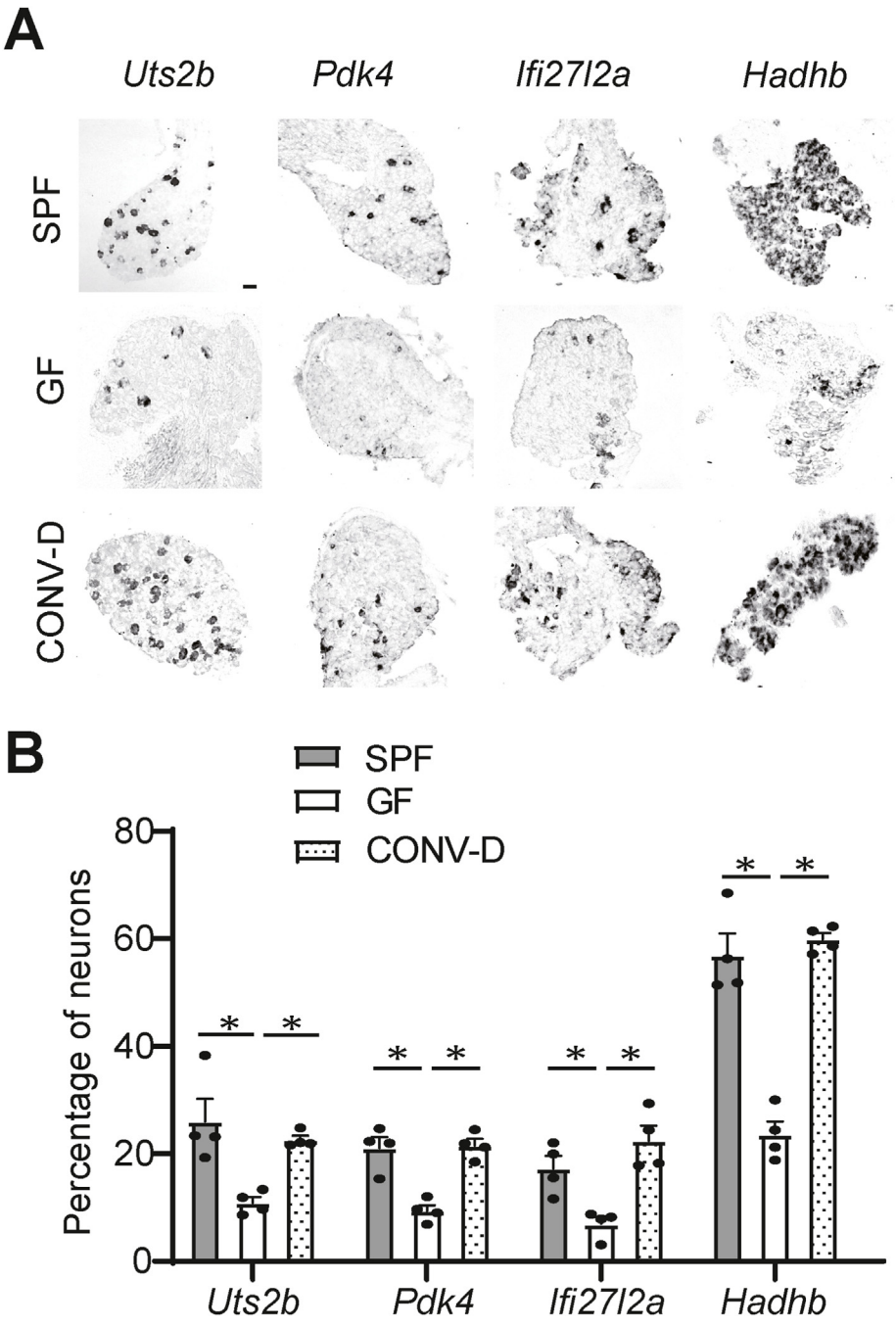

Fig. 1. Microbiota-dependent expression of the *Uts2b*, *Pdk4*, *Ifi27l2a* and *Hadhb* gene (A) Representative images of in situ hybridization signals. (B) Bar graph showing the percentage of signal-positive neuronal profiles in all NPG neurons. Results are shown as the mean ± SEM (n = 4 mice per condition). *p < .05; assessed with Mann-Whitney *U* test. Scale bar represents 50 μm.

in situ hybridization analysis (Fig. 1A). These analyses identified four genes (Supplemental Fig. 1D), *Uts2b, Pdk4, Ifi27l2a* and *Hadhb*, as genes whose expression in the NPG neurons was reduced in GF (as compared to SFP) and restored in CONV-D mice. (Fig. 1A and B). The *Uts2b, Pdk4, Ifi27l2a, and Hadhb* genes encode urotensin 2B (UTS2B) [13], pyruvate dehydrogenase kinase 4 [14], interferon α-inducible protein 27-like protein 2a [15], and hydroacyl-CoA dehydrogenase β [16], respectively. Quantification of neuronal profiles expressing those genes revealed nearly complete restoration of the neuronal numbers in the NPG of CONV-D mice (Fig. 1B), suggesting that GF condition reduces the expression of those genes in individual NPG neurons without affecting their survival.

We examined whether expression of those genes can be altered by microbiota-derived stimuli. The NPG from SPF mice were cultured in collagen gels and treated with AR420626 (a selective agonist of free fatty acid receptor 3: FFAR3), LPS (a ligand for Toll Like Receptor 4: TLR4) or Pam3CSK4 (a synthetic ligand for TLR2/3). RNAs extracted from the NPG were examined by qRT-PCR. AR420626 treatment increased the expression of *Uts2b* and *Pdk4*, but not *Ifi27l2a* and *Hadhb* (Fig. 2A). Treatment with LPS or Pam3CSK4 did not alter the expression of any of those genes (Fig. 2B and C). In situ hybridization analysis on the NPG revealed that the numbers of neurons expressing *Uts2b* and *Pdk4* were larger in AR420626-treated NPG than untreated controls. These data suggest that the NPG neurons respond to metabolites of microbiota and maintain and/or induce the expression of *Uts2b* and *Pdk4*.

Because enteroendocrine cells (EECs) sense microbiota and their metabolites and secret hormones, we further examined the effect of the intestinal hormones on the expression of *Uts2b* and *Pdk4* in cultured NPG. We focused on CCK, PYY and GLP-1 because previous studies suggested the involvement of the vagal nerves in functions of these intestinal hormones [17–19]. Although GLP-1 treatment decreased *Uts2b* expression, CCK treatment significantly upregulated its expression. PYY treatment displayed no effect on *Uts2b* expression (Fig. 3A–E). In contrast, treatment with any of these hormones did not influence the expression of *Pdk4*, *Ifi27l2a* and *Hadhb* (Fig. 3F and G, data not shown).

Consistent with these effects of intestinal hormones on *Uts2b* expression, *Cckar*, the receptor for CCK, and *Glp1r*, the receptor for GLP-1, were expressed in the majority (approximately 80%) of *Uts2b*-expressing NPG neurons (Supplemental Fig. 2A). On the other hand, only 20–25% of *Cckar* or *Glp1r*-expressing neurons expressed *Uts2b* (Supplemental Fig. 2A). *Npy2r*, the receptor for PYY, was expressed in a smaller population (about 40%) of *Uts2b*-expressing NPG neurons (Supplemental Fig. 2A). In contrast, those hormone receptors were barely expressed in *Pdk*-expressing NPG neurons (Supplemental Fig. 2B). Collectively, these data revealed differential regulation of *Uts2b* expression in NPG neurons by distinct intestinal hormones.

Significant induction of *Uts2b* expression in NPG neurons by CCK treatment prompted us to examine nerve projections of *Uts2b*-expressing NPG neurons in the gastrointestinal tract. We employed the dual genetic recombination system using the Ai65 reporter and selectively labeled *Uts2b*-expressing NPG neurons with tdTomato fluorescence. For the dual recombination, we used the *Vip-Cre* allele because 90% of *Vip*-expressing neurons express *Uts2b* (Supplemental Fig. 3A) [7] and the *Slc17a6-Flpo* allele because it drives recombination in almost all sensory neurons projecting to

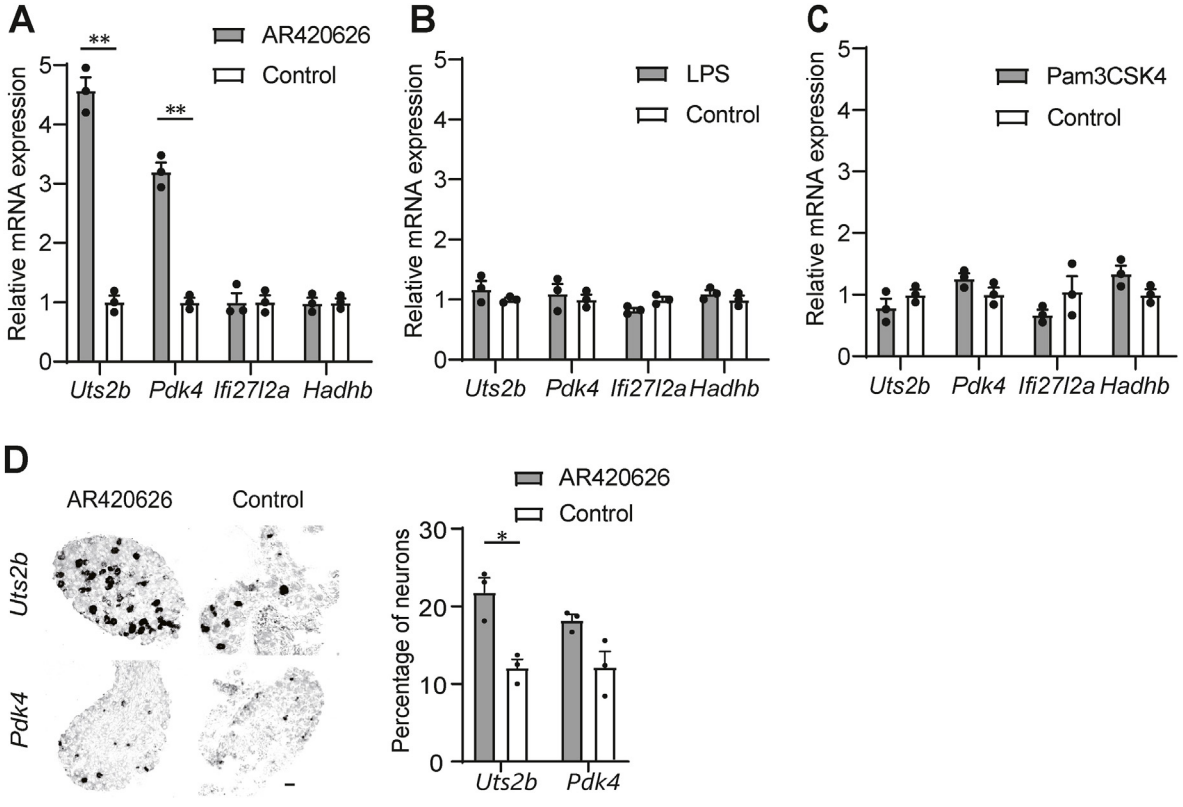

Fig. 2. Gene responses of NPG neurons to microbiota-derived extracellular signals. (A–C) Graphs showing results of the qRT-PCR analysis on the expression of the *Uts2b*, *Pdk4*, *Ifi27l2a* and *Hadhb* genes in the cultured NPG after treatment with AR420626 (A), LPS (B) and Pam3CSK4 (C). Bars indicate the relative levels of mRNA expression compared to untreated controls (assigned as 1). Three NPG were examined per treatment. (D) Representative images of in situ hybridization analysis using *Uts2b* and *Pdk4* riboprobes (left). Bar graph shows the percentage of signal-positive neurons in all NPG neurons (n = 3 mice per treatment). Results of qRT-PCR shown as the mean ± SEM. *p < .01, **p < .001; assessed with unpaired *t*-test with Welch's correction. Quantification of in situ hybridization (Percentage of neurons) shown as the mean ± SEM. *p < .05, assessed with Mann-Whitney *U* test. Scale ba; 50 μm.

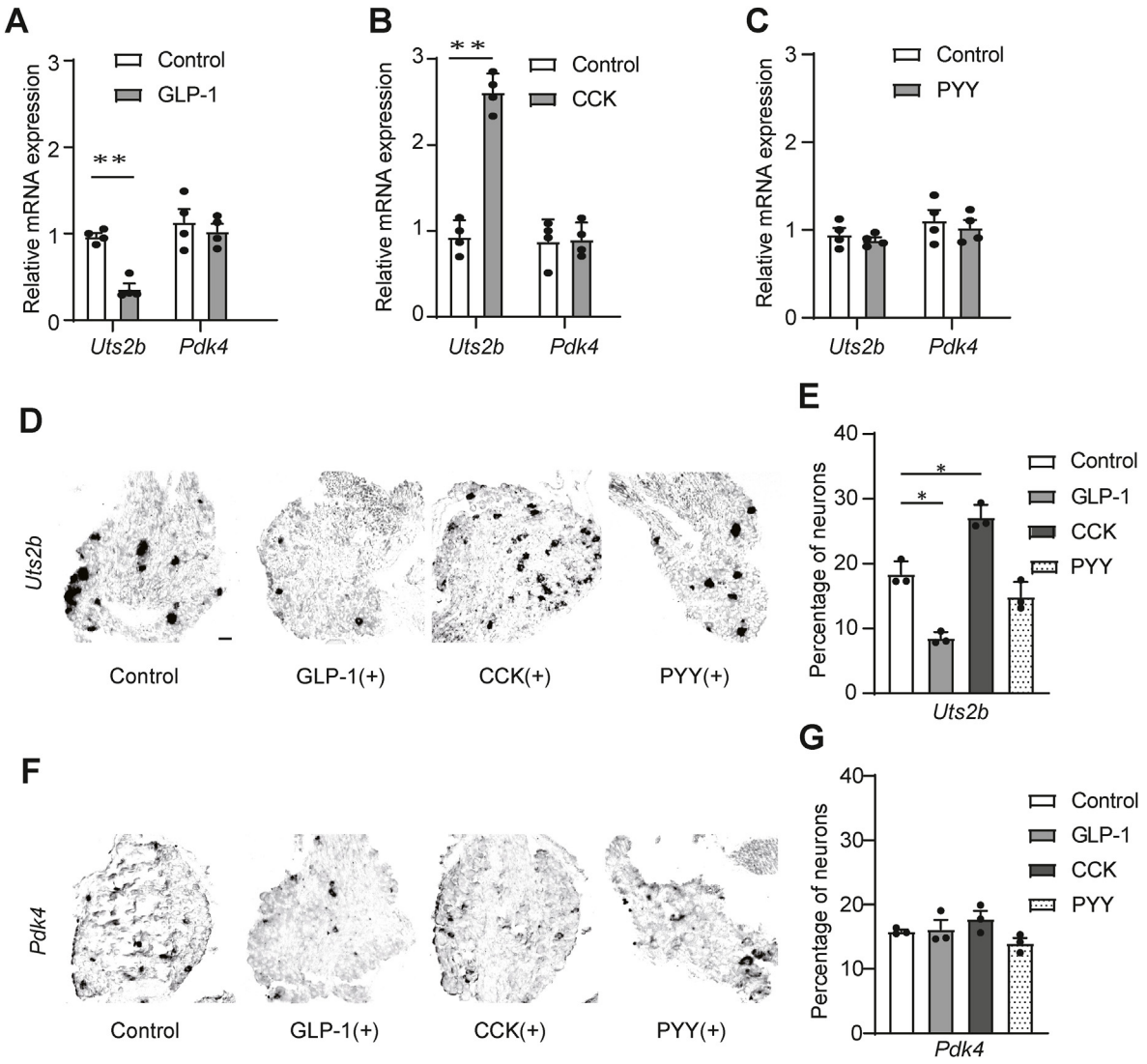

Fig. 3. Effects of intestinal hormones on the expression of the *Uts2b* and *Pdk4* gene in NPG neurons. (A–C) Graphs showing results of the qRT-PCR analysis on the expression of the *Uts2b* and *Pdk4* in the cultured NPG after treatment with 10 μM of GLP-1 (A), CCK (B) and PYY (C). (D–G) In situ hybridization analysis of *Uts2b* and *Pdk4* expression. (D and F) Representative images of in situ hybridization analysis using *Uts2b* and *Pdk4* riboprobes (E and G). Bar graphs show the percentage of positive neurons in all NPG neurons (n = 3 mice per treatment). Results of quantitative PCR are shown as the mean ± SEM. **p < .001; assessed with unpaired *t*-test with Welch's correction. Quantification results of in situ hybridization are shown as the mean ± SEM. *p < .05, assessed with Mann-Whitney *U* test. Scale bar: 50 μm.

the peripheral tissues [7]. To confirm the specificity of this labeling, we also injected Cre-dependent tdTomato expressing adeno-associated virus serotype 9 (AAV9-FLEX-tdT) to the NPG of *Vip-Cre* mice (Supplemental Figs. 3B and C). Both of these labeling methods provided essentially the same results, although the dual recombination system provided more comprehensive labeling. We found that tdTomato-positive nerve fibers were most abundant in the duodenum and upper jejunum but almost absent in the stomach (Supplemental Fig. 4D). In the duodenum and jejunum, the nerve fibers projected up to the mucosa lying beneath the epithelial layer of the villi (lamina propria). Such projection was observed in about one third of all the villi (Fig. 4B and C). Immunohistochemical staining with anti-CCK antibody revealed that td-Tomato-positive nerves were occasionally very close to (Fig. 4D) and Supplemental Fig. 3E) or in direct contact with CCK-expressing EECs at their neuropod-like basal protrusions (Fig. 4E, arrowhead, Supplemental Movie 1). These histological data support a tight biological link between *Uts2b*-expressing NPG neurons and CCK-expressing EECs.

Supplementary video related to this article can be found at https://doi.org/10.1016/j.bbrc.2022.03.117

4. Discussion

In this study, we discovered that the *Uts2b* gene is expressed by a subset of vagal afferent neurons in a microbiota-dependent manner and that its expression was increased by the selective agonist for FFAR3 and CCK. The direct contact between CCK-expressing EECs and nerve fibers of *Uts2b*-expressing vagal afferent neurons strongly suggests that those neurons are responsible for relaying sensory information from CCK-expressing EECs.

Distinct populations of vagal afferent neurons project to different regions in the gut [20]. Our genetic labeling of *Uts2b*-expressing NPG neurons revealed that their dendritic nerve fibers project to the lamina propria of the villi, which are located closest, among all the vagal afferent projections, to the gut surface. This observation suggests that *Uts2b*-expressing NPG neurons are ready to sense the gut luminal environment, which is consistent with our

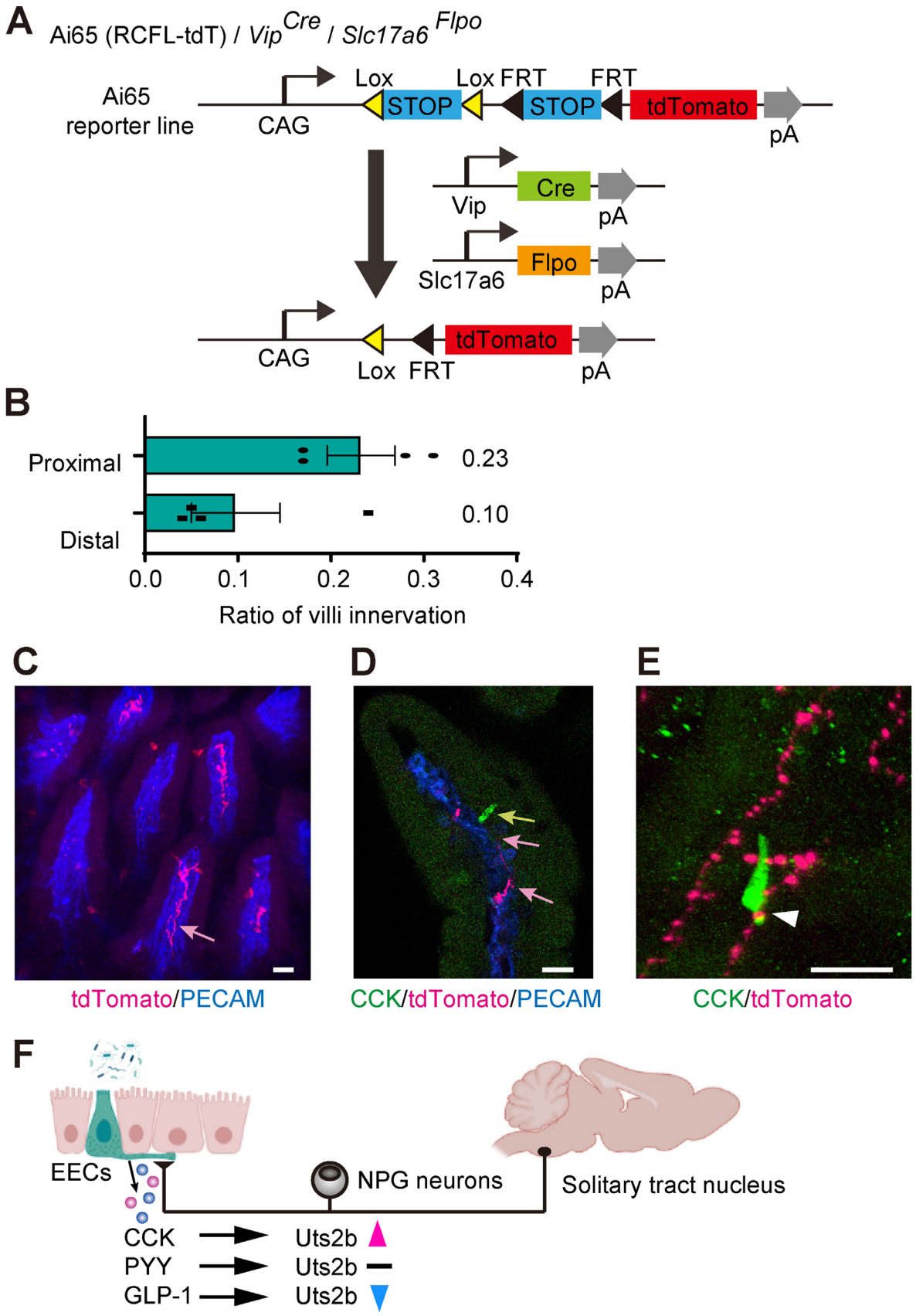

Fig. 4. CCK $^{+}$ enteroendocrine cells make contact with VIP $^{+}$ vagal neurons. (A) Ai65 (RCFL-tdT) allele used for intersectional genetic labeling of Vip^{+} and vGlut2+ (Slc17a6^{+}) neurons. (B) Quantification of mucosal ending-distributions of Vip^{+}-vGlut2^{+} neurons (mean ± SEM) in the proximal and distal small intestine. (C) Representative image showing mucosal endings of Vip^{+}-vGlut2^{+} neurons. (D) Representative confocal image showing CCK^{+} enteroendocrine cell (green, yellow arrow) and Vip^{+}-vGlut2^{+} nerve mucosal ending (magenta, pink arrows) in the small intestine. (E) Reconstructed 3D confocal image showing CCK^{+} enteroendocrine cell (green) contacting Vip^{+}-vGlut2^{+} nerve fiber (magenta) innervating the mucosa of the small intestine. White arrowhead indicates the contact site between CCK^{+} enteroendocrine cell and Vip^{+}-vGlut2^{+} nerve fiber. (F) Model of intestinal sensing by enteroendocrine cells and Uts2b^{+} vagal afferents. *Uts2b* expression in NPG neurons is differently regulated by CCK, PYY and GLP-1 from enteroendocrine cells. The Scale bars, 20 μm.

observation that *Uts2b* expression is upregulated by FFAR3 agonist and CCK. The mode of activation of *Uts2b*-expressing vagal neurons can therefore be determined by combined effects of direct (bacterial metabolites) and indirect (gut hormones) pathways.

Although the physiological role of UTS2B is currently unknown, previous studies showed that it signals through the urotensin 2 receptor (UTS2R) and the somatostatin receptor 5 (SSTR5), both of which are G protein-coupled receptors (GPCRs). Because activation of GPCR in neurons can influence their neurotransmission [21], UTS2B may function as a neuromodulator in neural transduction from vagal afferent neurons to neurons in the nucleus of the solitary tract (NTS).

Single cell RNA sequencing analyses of the mouse gut epithelium demonstrated that a single class of EEC expresses more than one intestinal hormone, and a subpopulation of CCK-expressing EECs co-express PYY and GLP-1 [22]. Because Uts2b expression in vagal afferent neurons is differentially altered by CCK, GLP-1 and PYY, different levels of UTS2B can lead to distinct patterns of neuronal excitation in the NTS. In this manner, UTS2B may contribute to modulation of gut sensory modality emanating from EECs (Fig. 4F).

Although CCK is a well-known anorexigenic hormone [1,2], a recent study revealed a role of CCK in nutrient preference [6]. CCK-expressing EECs are connected to two distinct types of vagal afferent neurons, glutamatergic and purinergic, which transduce sensation of sugar and sweetener, respectively. Importantly, sugar sensation is dependent on not only glutamate but also CCK [6]. Thus, CCK is a multifunctional hormone that influences distinct animal behaviors. Because Uts2b-expressing neurons constitute only 25% of CCK-A expressing vagal afferent neurons, UTS2B may contribute to determining the mode of CCK's actions such as sugar sensation. Elucidating the role of UTS2B awaits genetic engineering that disrupts the *Uts2b* gene in a vagal afferent neuron-specific manner.

Declaration of competing interest

The authors declare that they have no known competing financial interests or personal relationships that could have appeared to influence the work reported in this paper.

Acknowledgements

This research is supported by Japan Science and Technology Agency and MEXT and AMED under the Grant Number JPMJCR2021 and JP21dm0207111.

Appendix A. Supplementary data

Supplementary data to this article can be found online at https://doi.org/10.1016/j.bbrc.2022.03.117.

References

[1] F.M. Gribble, F. Reimann, Enteroendocrine cells: chemosensors in the intestinal epithelium, Annu. Rev. Physiol. 78 (2016) 277–299, https://doi.org/10.1146/annurev-physiol-021115-105439.

[2] J. Beumer, J. Puschhof, J. Bauza-Martinez, A. Martinez-Silgado, R. Elmentaite, K.R. James, A. Ross, D. Hendriks, B. Artegiani, G.A. Busslinger, B. Ponsioen, A. Andersson-Rolf, A. Saftien, C. Boot, K. Kretzschmar, M.H. Geurts, Y.E. Bar-Ephraim, C. Pleguezuelos-Manzano, Y. Post, H. Begthel, F. van der Linden, C. Lopez-Iglesias, W.J. van de Wetering, R. van der Linden, P.J. Peters, A.J.R. Heck, J. Goedhart, H. Snippert, M. Zilbauer, S.A. Teichmann, W. Wu, H. Clevers, High-resolution mRNA and secretome atlas of human enteroendocrine cells, Cell 182 (2020) 1062–1064, https://doi.org/10.1016/j.cell.2020.08.005.

[3] M.M. Kaelberer, K.L. Buchanan, M.E. Klein, B.B. Barth, M.M. Montoya, X. Shen, D.V. Bohorquez, A gut-brain neural circuit for nutrient sensory transduction, Science 361 (2018), https://doi.org/10.1126/science.aat5236.

[4] D.V. Bohorquez, R.A. Shahid, A. Erdmann, A.M. Kreger, Y. Wang, N. Calakos, F. Wang, R.A. Liddle, Neuroepithelial circuit formed by innervation of sensory enteroendocrine cells, J. Clin. Invest. 125 (2015) 782–786, https://doi.org/10.1172/JCI78361.

[5] F.M. Gribble, F. Reimann, Function and mechanisms of enteroendocrine cells and gut hormones in metabolism, Nat. Rev. Endocrinol. 15 (2019) 226–237, https://doi.org/10.1038/s41574-019-0168-8.

[6] K.L. Buchanan, L.E. Rupprecht, M.M. Kaelberer, A. Sahasrabudhe, M.E. Klein, J.A. Villalobos, W.W. Liu, A. Yang, J. Gelman, S. Park, P. Anikeeva, D.V. Bohorquez, The preference for sugar over sweetener depends on a gut sensor cell, Nat. Neurosci. 25 (2022) 191–200, https://doi.org/10.1038/s41593-021-00982-7.

[7] L. Bai, S. Mesgarzadeh, K.S. Ramesh, E.L. Huey, Y. Liu, L.A. Gray, T.J. Aitken, Y. Chen, L.R. Beutler, J.S. Ahn, L. Madisen, H. Zeng, M.A. Krasnow, Z.A. Knight, Genetic identification of vagal sensory neurons that control feeding, Cell 179 (2019) 1129–1143, https://doi.org/10.1016/j.cell.2019.10.031, e1123.

[8] M. Fukuchi, A. Tabuchi, Y. Kuwana, S. Watanabe, M. Inoue, I. Takasaki, H. Izumi, A. Tanaka, R. Inoue, H. Mori, H. Komatsu, H. Takemori, H. Okuno, H. Bito, M. Tsuda, Neuromodulatory effect of Galphas- or Galphaq-coupled G-protein-coupled receptor on NMDA receptor selectively activates the NMDA receptor/Ca2+/calcineurin/cAMP response element-binding protein-regulated transcriptional coactivator 1 pathway to effectively induce brain-derived neurotrophic factor expression in neurons, J. Neurosci. 35 (2015) 5606–5624, https://doi.org/10.1523/JNEUROSCI.3650-14.2015.

[9] H. Taniguchi, M. He, P. Wu, S. Kim, R. Paik, K. Sugino, D. Kvitsiani, Y. Fu, J. Lu, Y. Lin, G. Miyoshi, Y. Shima, G. Fishell, S.B. Nelson, Z.J. Huang, A resource of Cre driver lines for genetic targeting of GABAergic neurons in cerebral cortex, Neuron 71 (2011) 995–1013, https://doi.org/10.1016/j.neuron.2011.07.026.

[10] H. Enomoto, I. Hughes, J. Golden, R.H. Baloh, S. Yonemura, R.O. Heuckeroth, E.M. Johnson Jr., J. Milbrandt, GFRalpha1 expression in cells lacking RET is dispensable for organogenesis and nerve regeneration, Neuron 44 (2004) 623–636, https://doi.org/10.1016/j.neuron.2004.10.032.

[11] K.K. Ishii, T. Osakada, H. Mori, N. Miyasaka, Y. Yoshihara, K. Miyamichi, K. Touhara, A labeled-line neural circuit for pheromone-mediated sexual behaviors in mice, Neuron 95 (2017) 123–137, https://doi.org/10.1016/j.neuron.2017.05.038, e128.

[12] H. Enomoto, T. Araki, A. Jackman, R.O. Heuckeroth, W.D. Snider, E.M. Johnson Jr., J. Milbrandt, GFR a1-deficient mice have deficits in the enteric nervous system and kidneys, Neuron 21 (1998) 317–324.

[13] C. Tang, I. Ksiazek, N. Siccardi, B. Gapp, D. Weber, J. Wirsching, V. Beck, M. Reist, L. Gaudet, N. Stuber, S.S. Surber, X. Mao, T.B. Nicholson, W. Carbone, M. Beibel, G. Roma, C. Gubser Keller, F. Bassilana, UTS2B defines a novel enteroendocrine cell population and regulates GLP-1 secretion through SSTR5 in male mice, Endocrinology 160 (2019) 2849–2860, https://doi.org/10.1210/en.2019-00549.

[14] R.S. Alqurashi, A.S. Yee, T. Malone, S. Alrubiaan, M.W. Tam, K. Wang, R.R. Nandedwalla, W. Field, D. Alkhelb, K.S. Given, R. Siddiqui, J.D. Baleja, K.E. Paulson, A.S. Yee, A Warburg-like metabolic program coordinates Wnt, AMPK, and mTOR signaling pathways in epileptogenesis, PLoS One 16 (2021), e0252282, https://doi.org/10.1371/journal.pone.0252282.

[15] T.M. Lucas, J.M. Richner, M.S. Diamond, The interferon-stimulated gene Ifi27l2a restricts west nile virus infection and pathogenesis in a cell-type- and region-specific manner, J. Virol. 90 (2015) 2600–2615, https://doi.org/10.1128/JVI.02463-15.

[16] Y.B. Hong, J.H. Lee, J.M. Park, Y.R. Choi, Y.S. Hyun, B.R. Yoon, J.H. Yoo, H. Koo, S.C. Jung, K.W. Chung, B.O. Choi, A compound heterozygous mutation in HADHB gene causes an axonal Charcot-Marie-tooth disease, BMC Med. Genet. 14 (2013) 125, https://doi.org/10.1186/1471-2350-14-125.

[17] M. Kakei, T. Yada, A. Nakagawa, H. Nakabayashi, Glucagon-like peptide-1 evokes action potentials and increases cytosolic Ca2+ in rat nodose ganglion neurons, Auton. Neurosci. 102 (2002) 39–44, https://doi.org/10.1016/s1566-0702(02)00182-0.

[18] Y. Iwasaki, M. Kakei, H. Nakabayashi, E.A. Ayush, M. Hirano-Kodaira, Y. Maejima, T. Yada, Pancreatic polypeptide and peptide YY3-36 induce Ca2+ signaling in nodose ganglion neurons, Neuropeptides 47 (2013) 19–23, https://doi.org/10.1016/j.npep.2012.07.006.

[19] G.J. Dockray, Enteroendocrine cell signalling via the vagus nerve, Curr. Opin. Pharmacol. 13 (2013) 954–958, https://doi.org/10.1016/j.coph.2013.09.007.

[20] Y.B. Wang, G. de Lartigue, A.J. Page, Dissecting the role of subtypes of gastrointestinal vagal afferents, Front. Physiol. 11 (2020) 643, https://doi.org/10.3389/fphys.2020.00643.

[21] H.T. Huang, P.C. Chen, P.S. Chen, W.T. Chiu, Y.M. Kuo, S.F. Tzeng, Inhibitory effects of trifluoperazine on peripheral proinflammatory cytokine expression and hypothalamic Microglia activation in obese mice induced by chronic feeding with high-fat-diet, Front. Cell. Neurosci. 15 (2021) 752771, https://doi.org/10.3389/fncel.2021.752771.

[22] A.L. Haber, M. Biton, N. Rogel, R.H. Herbst, K. Shekhar, C. Smillie, G. Burgin, T.M. Delorey, M.R. Howitt, Y. Katz, I. Tirosh, S. Beyaz, D. Dionne, M. Zhang, R. Raychowdhury, W.S. Garrett, O. Rozenblatt-Rosen, H.N. Shi, O. Yilmaz, R.J. Xavier, A. Regev, A single-cell survey of the small intestinal epithelium, Nature 551 (2017) 333–339, https://doi.org/10.1038/nature24489.